IIETA International Information and Engineering Technology Association
Advancing the World of Information and Engineering

Mathematical Modelling of Engineering Problems
Vol. 11, No. 4, April, 2024, pp. 1053-1059
Journal homepage: http://iieta.org/journals/mmep

Hydrolytic Aging of Wire Enameled with Polyesterimide and Polyamide Imide Used in Electrical Machines

Fatima Kerkarine, Mohammed Nedjar*

Laboratoire de Génie Electrique, Université Mouloud Mammeri, Tizi-Ouzou 15000, Algeria

Corresponding Author Email: mohammed.nedjar@ummto.dz

https://doi.org/10.18280/mmep.110423

Received: 15 October 2023
Revised: 7 January 2024
Accepted: 20 January 2024
Available online: 26 April 2024

Keywords:
hydrolytic aging, polyesterimide, polyamide imide, breakdown voltage, TGA, FTIR, Weibull statistic

ABSTRACT

This paper reports the influence of hydrolytic aging on the rupture voltage of copper wire enameled with polyestermide reinforced by a polyamide imide layer. A large population of samples was put in a climatic chamber regulated at 40°C and 93% relative humidity. The wet aging was carried out until 15000h. Every time of 500h, 80 samples were taken from the climatic chamber and submitted to AC breakdown test. A statistic investigation of breakdown voltage values was done using Weibull model. Scale parameter, shape parameter and confidence intervals are presented. The breakdown voltage changes in function of aging time. The raise is ascribed to the arrangement in the structure of the polymer. While its lowering is assigned to the diminution in the viscosity causing a raise of mean free path of charge carriers. The shape parameter changes versus aging time. The shortening is due to the increase in the size of defects. Whereas its raise is allotted to the arrangement in the structure. TGA shows a variation of the onset temperature and the residue during the aging. The FTIR tests show a weak modification of the spectra. There is no degradation of the insulation, however a change in molecular conformation occurs. The results are analyzed and discussed.

1. INTRODUCTION

Polymers are extensively employed in electric apparatus (cables, generators, transformers, motors, etc.) because of their excellent electrical and mechanical properties. During their service, polymeric materials are expected to work under the action of moisture. It was indicated that the water content of cable XLPE insulation, after 17778h of immersion in water at 80°C, attained 4000ppm [1]. In electric cable, water can be put during the production, transportation, stocking, laying, service, etc. as mentioned by Nikolajevic [2]. Baschek et al. [3] yielded that water absorption is affected by temperature, time of immersion, thickness of sample, and the amorphous part in a polymer. These researchers indicated that the saturated water contents in polymers vary between 0.3wt% (polycarbonate) and 10wt% (polyamide). Under electric field, the presence of moisture causes poor performance of dielectric materials and can induce rupture by water treeing [4]. Numerous works highlighted the alteration of polymers submitted to hydrolytic aging [5-9].

In a preceding investigation [5], we studied the action of moisture on the breakdown voltage of polyesterimide used in electric motors. The samples were exhibited to 90% relative humidity and 30°C during 3000h. This investigation shows that the breakdown voltage is altered by the aging.

In another work [6], we investigated the variation of the electrical properties of crosslinked polyethylene (XLPE) under the action of moisture. The specimens were exhibited to 100% relative humidity and ambient temperature until 5600h. The study pointed a change in dielectric loss factor, permittivity, volume resistivity and dielectric strength.

The action of moisture on the dielectric strength of polyamide (aramid) paper was viewed by UI-Haq [7]. Samples were aged in water at 23°C. The author indicated a change of 12.2% in the polymer weight for duration of 2400h (100 days). It was reported a reduction in breakdown strength from 57.96MV/m to 13.11MV/m after aging.

Chauvet et al. [8] examined the influence of humidity on the breakdown strength of XLPE cable. The samples were aged at ambiant temperature, under electric field of 25kV/mm in the presence of water. Baschek et al. [3] found that the water content in the samples changes between 50 and 400ppm before aging and after 720h, respectively. These researchers reported that the wet aging affects the breakdown field of XLPE.

Diaz et al. [9] examined the hydrolytic aging of a thermoplastic polyether ester elastomer (TPEs). The samples thermoplastic polyether were placed in water at 98°C. The authors mentioned that the wet aging induces a raise in cristallinity, and a lessening of tensile strength and strain.

This work focuses on the actions of hydrolytic aging on the breakdown voltage of an insulation composed by polyesterimide and polyamide imide. The use of wires enameled with polyesterimide and polyamide imide has raised quickly because of their excellent resistance to high temperatures, good electrical and chemical properties [10]. The dielectric material is characterized by TGA and FTIR.

2. EXPERIMENTS

2.1 Samples

A spool of enameled copper wire was supplied by "TREFICUIVRE" maker in Algeria". The diameter of the conduteurs is 0.63mm. The insulation, having a thickness of 33µm, is composed by polyesterimide covered with a thin layer of polyamide imide. The insulation is of class C (200°C).

The samples were performed as a bended copper conductor in agreement with the IEC 60851-5 Standard [11]. The length of the samples is 125mm. A twist includes 12 turns of wire. To avoid bypasses during the experiment of dielectric rupture, the extremities of the specimens were separated. In order to detect any presence of cracks, the samples were checked with a microscope.

2.2 Hydrolytic aging

A large number of samples were introduced in a climatic chamber regulated at 93% relative humidity and a temperature of 40°C. The aging time attained 15000h (625 days). After every aging time of 500h, a sampling of 80 specimens was taken from the climatic chamber.

2.3 Dielectric breakdown test

The samples were submitted to dielectric breakdown by applying an AC voltage of 50Hz frequency, with a velocity of 0.5kV/s. The experiments were accomplished in air, at room temperature. The values of the rupture voltage were recorded.

2.4 Characterization

2.4.1 Thermal gravimetric analysis

The thermal gravimetric analysis (TGA) was controlled with NETZSCH STA 409 PC/PG at temperatures locating between 40 to 1000°C under a nitrogen atmosphere. A powder was slowly withdrawn from the enameled wire and placed in a crucible. The warming speed is 10°C/min and programmed with a computer. The average mass of the specimens is 1.5mg.

2.4.2 Fournier transform infrared spectroscopy

The insulating material was also examined by Fournier transform infrared spectroscopy (FTIR). Infrared spectra were carried out on JASCO FT/IR in the wavenumber between 4000-500cm^{-1}. The device is connected to a computer.

3. STATISTICAL ANALYSIS OF BREAKDOWN VOLTAGE DATA

The obtained values of failure voltage were analysed using Weibull statistic. This last is widely used to treat breakdown statistic data of solid insulating materials [12-16]. The two-parameter Weibull distribution is yielded by the following formula [17]:

$$P(V)=1-\exp\left[-\left(\frac{V}{V_O}\right)\right]^{\beta} \quad (1)$$

where,

P(V): cumulative probability;

V: rupture voltage;

V_0: scale parameter that is the value of V corresponding to a cumulative probability of 63.2%;

β: shape parameter which is the incline of the straight line of Weibull plot.

The different stages of the statistical investigation are displayed below:

The cumulative failure probability P_i was calculated, for P_i was each value of V_i, by the following expression [18]:

$$P_i = \frac{i}{N+1}100\% \quad (2)$$

with,

i: rank of V_i after a classification by ascending order;

N: total number of samples. In this study, N=80 specimens.

The graph, representing $\log \ln\left(\frac{1}{1-P_i}\right)$ in function of $\log V_i$, was plotted. The Weibull plots were executed by fitting the breakdown data using the maximum likelihood method. The calculation was performed employing a computer program elaborated by "Laboratoire de Génie Electrique de Toulouse, France" currently "LAPLACE". The best straight line was chosen. The values of V_0 and β were deduced. Jacquelin [19] reported that this method is generalized to deal data of dielectric failure.

The 90% confidence intervals were established employing the maximum likelihood method. In this case, we fix a risk of 10% to find an experimental point, belonging to the true distribution, outside the tolerance intervals.

4. RESULTS AND DISCUSSION

4.1 Statistical analysis

Tables 1-3 presented the values of the nominal breakdown voltage (or scale parameter), the shape parameter, the equations of Weibull plots, and the confidence intervals. For more convenience, only the Weibull plots, matching to unaged samples, and those aged after 5000h, 10000h and 15000h, will be exposed in Figure 1 (a-d).

4.2 Change of breakdown voltage in function of aging time

Figure 2 shows the changing of rupture voltage (V_0) versus aging time. As one can see, the figures display an irregular development with the presence of various peaks. The variation can be described after:

- At the first, failure voltage decreases from 12.71kV to 9.85kV, rises to 10.50kV corresponding to 1000h. Afterwards V_0 lessens to 8.11kV and grows until 10.72kV for 3000h. Beyond, V_0 shortens to 8.05kV and augments until 8.98kV for 5500h.
- Next, V_0 decreases to 8.04kV and rises to 9.01kV corresponding to 6500h and remains somewhat constant. After 7500h, V_0 diminishes to 7.87kV, rises and reaches 9.97kV then decreases rapidly to 7.29kV for 10000h.
- Afterwards, V_0 grows to 9.10kV, and shortens to 7.30kV for 11500h. Beyond this time, it enhances to 9.47kV, shortens to 9.04kV and remains somewhat invariable. After 13500h, the breakdown voltage lowers rapidly to 6.14kV corresponding to 15000h.
- The maximum variation of the breakdown voltage is 51.69%.

Table 1. Confidence intervals of breakdown voltage

Aging Time (h)	Breakdown Voltage (kV)
0	12.368<V_0=12.709<13.056
500	9.385<V_0=9.845<10.322
1000	10.062<V_0=10.499<10.950
1500	8.472<V_0=8.888<9.319
2000	7.603<V_0=8.108<8.640
2500	9.252<V_0=9.716<10.198
3000	10.288<V_0=10.720<11.165
3500	9.739<V_0=10.164<10.602
4000	9.009<V_0=9.473<9.955
4500	7.655<V_0=8.050<8.460
5000	8.215<V_0=8.660<9.124
5500	8.597<V_0=8.978<9.371
6000	7.630<V_0=8.041<8.469
6500	8.671<V_0=9.010<9.358
7000	8.545<V_0=8.982<9.436
7500	8.389<V_0=8.895<9.425
8000	7.381<V_0=7.866<8.376
8500	8.630<V_0=9.099<9.588
9000	9.517<V_0=9.967<10.433
9500	7.933<V_0=8.400<8.900
10000	6.743<V_0=7.286<7.866
10500	6.777<V_0=7.455<8.192
11000	8.660<V_0=9.101<9.559
11500	6.723<V_0=7.299<7.917
12000	9.011<V_0=9.466<9.938
12500	8.605<V_0=9.042<9.496
13000	8.737<V_0=9.234<9.753
13500	8.652<V_0=9.178<9.73
14000	7.413<V_0=7.906<8.425
14500	7.602<V_0=8.093<8.610
15000	5.802<V_0=6.143<6.500

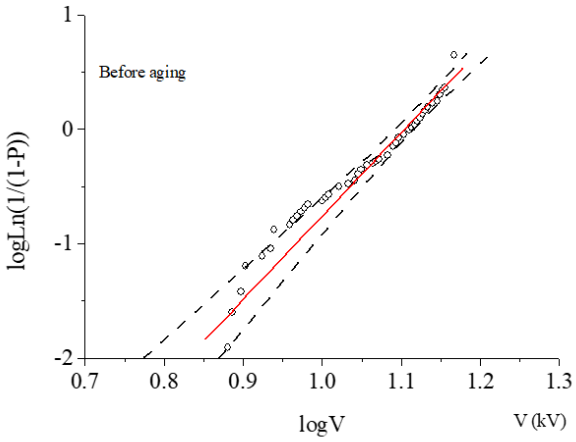

(a)

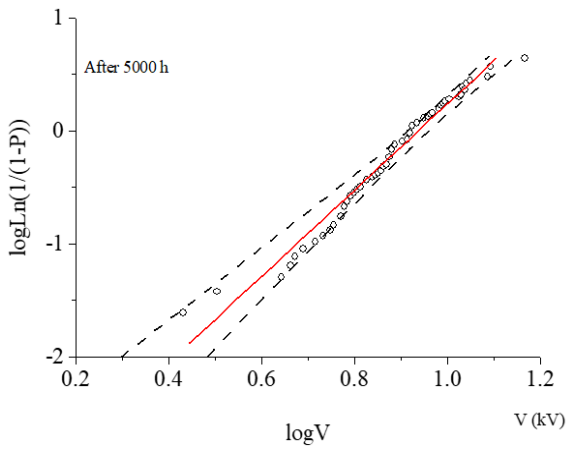

(b)

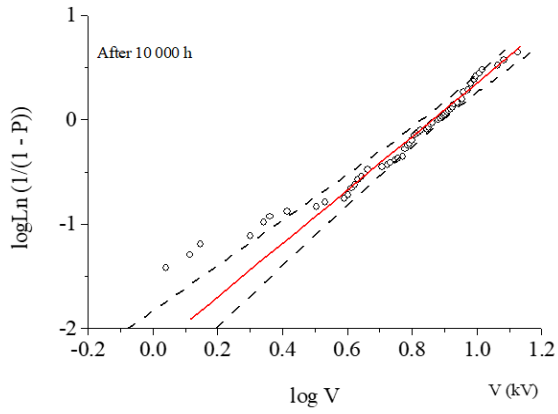

(c)

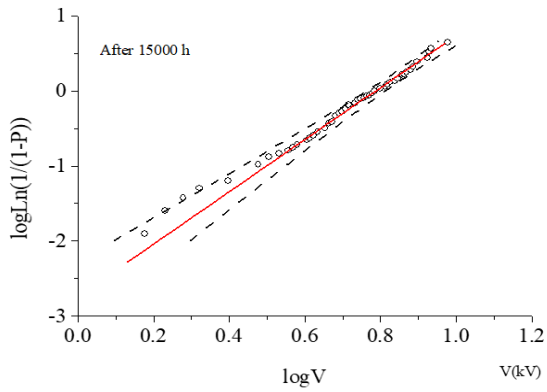

(d)

Figure 1. Weibull plot of breakdown voltage: (a) before aging; (b) after 5000h of aging; (c) after 10000h of aging; (d) after 15000h of aging

Table 2. Equations of Weibull graphs

Aging Time (h)	Equation of Weibull Plot
0	Y=7.294X-8.054
500	Y=4.146X-4.116
1000	Y=4.666X-4.764
1500	Y=4.140X-3.928
2000	Y=3.085X-2.803
2500	Y=4.056X-4.005
3000	Y=4.897X-5.045
3500	Y=4.613X-4.649
4000	Y=3.952X-3.839
4500	Y=3.947X-2.669
5000	Y=3.763X-3.528
5500	Y=4.578X-4.364
6000	Y=3.785X-3.426
6500	Y=5.172X-4.938
7000	Y=3.978X-3.793
7500	Y=3.391X-3.218
8000	Y=3.121X-2.796
8500	Y=3.746X-3.593
9000	Y=4.294X-4.288
9500	Y=3.391X-3.134
10000	Y=2.560X-2.208
10500	Y=2.081X-1.815
11000	Y=3.998X-3.835
11500	Y=2.413X-2.083
12000	Y=4.031X-3.935
12500	Y=4.007X-3.832
13000	Y=3.588X-3.464
13500	Y=3.362X-3.237
14000	Y=3.084X-2.769
14500	Y=3.169X-2.878
15000	Y=3.471X-2.737

Table 3. Confidence intervals of shape parameter

Aging Time (h)	Shape Parameter
0	6.151<β=7.294<8.352
500	3.496<β=4.146<4.747
1000	3.935<β=4.666<5.343
1500	3.491<β=4.140<4.740
2000	2.602<β=3.085<3.532
2500	3.420<β=4.056<4.644
3000	4.065<β=4.897<5.519
3500	3.884<β=4.613<5.287
4000	3.333<β=3.952<4.525
4500	3.328<β=3.947<4.519
5000	3.173<β=3.763<4.309
5500	3.861<β=4.578<5.242
6000	3.192<β=3.785<4.334
6500	4.361<β=5.172<5.922
7000	3.355<β=3.978<4.555
7500	2.860<β=3.391<3.883
8000	2.632<β=3.121<3.574
8500	3.159<β=3.746<4.289
9000	3.621<β=4.294<4.917
9500	2.860<β=3.391<3.883
10000	2.159<β=2.560<2.931
10500	1.755<β=2.081<2.383
11000	3.371<β=3.998<4.578
11500	2.035<β=2.413<2.763
12000	3.399<β=4.031<4.616
12500	3.379<β=4.007<4.588
13000	3.026<β=3.588<4.108
13500	2.835<β=3.362<3.850
14000	2.601<β=3.084<3.531
14500	2.672<β=3.169<3.629
15000	2.927<β=3.471<3.974

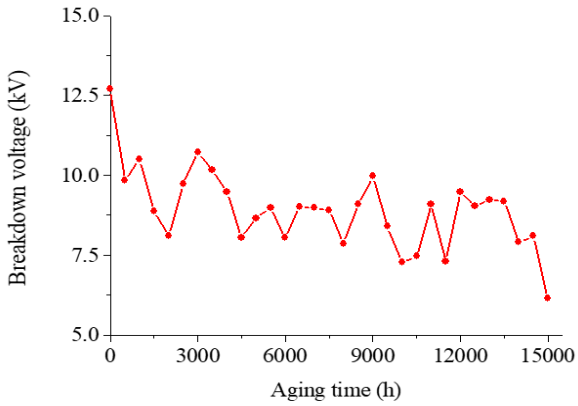

Figure 2. Breakdown voltage against aging time

4.3 Change of shape parameter against aging time

The dependence of aging time on shape parameter (β) is presented in Figure 3 which exhibits, like Figure 2, several peaks. The evolutions can be summed below:

- At the beginning of aging, the shape parameter lessens from 7.29 to 4.15 and rises to 4.67 for 1000h. Then it lowers to 3.09 and grows to 4.90 after 3000h. Afterwards it diminishes to 2.95 and increases to 4.58 corresponding to 5000h.
- After 5000h, β decreases to 3.79, increases to 5.17 and shortens to 3.12 corresponding to 8000h. Then it enhances to 4.29 and lessens to 2.08 after 10500h.
- Beyond 10500h, the shape parameter increases to 4.0 and decreases to 2.41 corresponding to 11500h. After this time, β augments to 4.03 and diminishes slowly to 3.08, and heightens slightly to 3.47 for 15000h.
- The maximum variation of shape parameter is 52.40%.

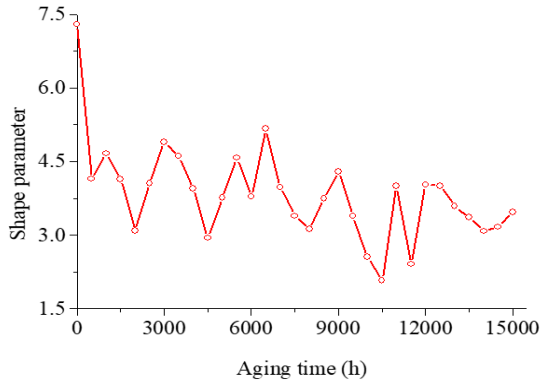

Figure 3. Shape parameter against aging time

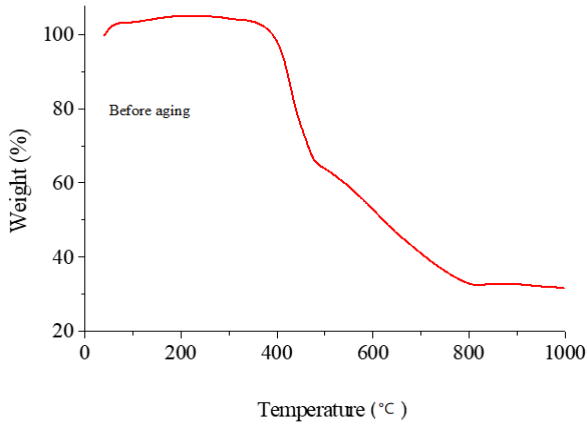

(a)

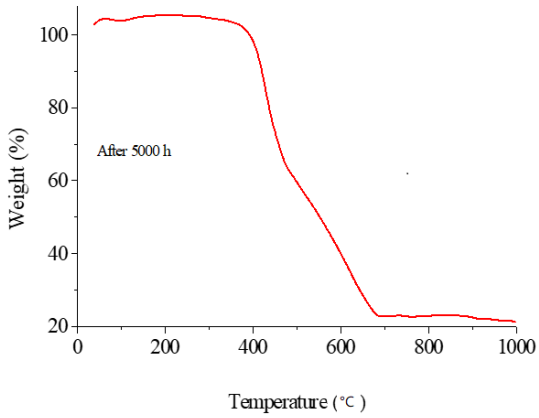

(b)

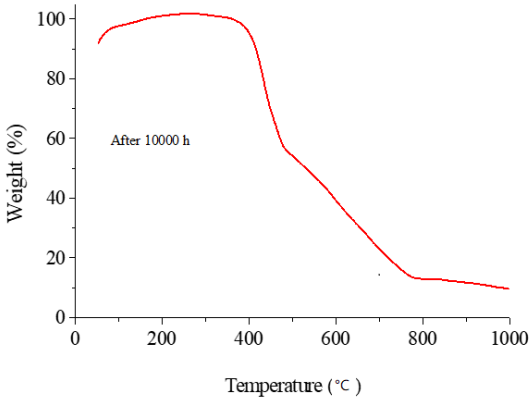

(c)

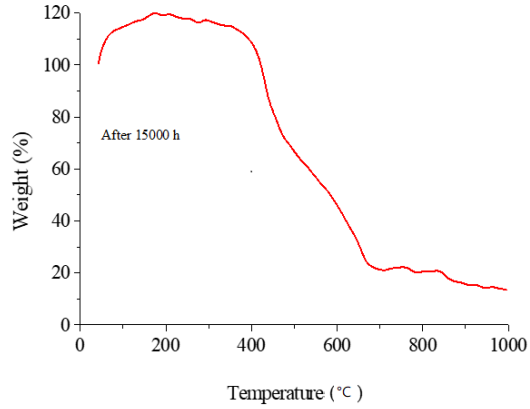

(d)

Figure 4. Thermogravimetric analysis curve: (a) before aging; (b) after 5000h of aging; (c) after 10000h of aging; (d) after 15000h of aging

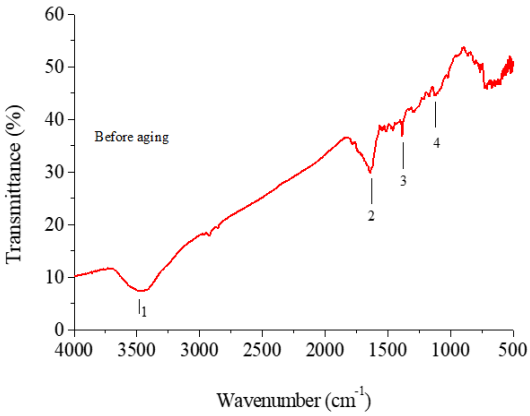

(a)

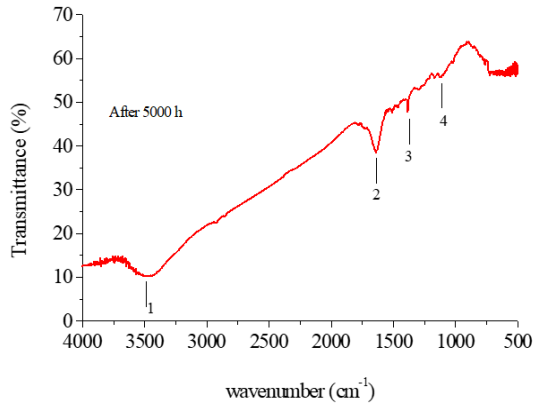

(b)

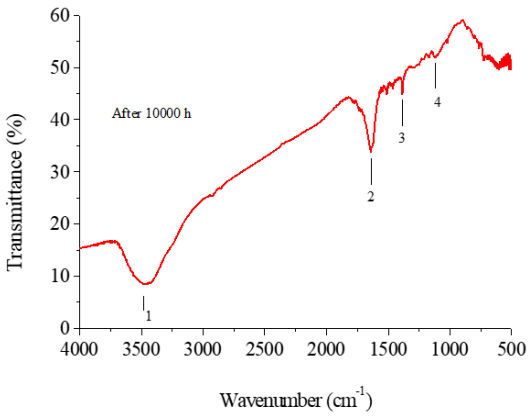

(c)

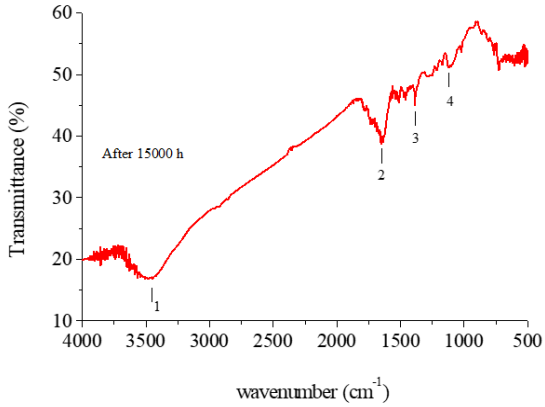

(d)

Figure 5. FTIR spectrum: (a) before aging; (b) after 5000h of aging; (c) after 10000h of aging; (d) after 15000h of aging

4.4 Thermal gravimetric analysis

The dependence of temperature on polymer weight is exposed in Figure 4 (a-d). The variations can be depicted as follows:

- In the range of the temperatures 100°C-400°C, a short increase in the weight is observed for all aging times. This raise is attributed to the oxydation of the dielectric material.
- Before aging, the weight loss initiates at about 406°C, accelerates and reaches 67.5% at 778°C, then it decelerates and it remains a residual of 32.0% at 997°C. The temperature of 50% weight loss is 623°C.
- Next 5000h, the weight loss begins at about 411°C. Beyond the onset temperature, it expedites and achieves 77.3% at 692°C. Next, the weight loss slackens and it rests a remnant of 21.0% at 997°C. The temperature of 50% weight loss is 552°C.
- After 10000h, the weight loss begins at around 403°C and quickens up to 87.6% for a temperature about 774°C. After, the weight loss decelerates and it remains a residuum of 9.3% at 999°C. The temperature of 50% weight loss is 531°C.
- After 15000h, the weight increases from 100% at 43°C to 119.6% corresponding to 176°C. Then it decreases slightly to 116.1% for 276°C. Afterwards, the weight raises a little and diminishes again to 100% for 422°C. From this point, the weight loss gets started and quickens up to 81.0% at 680°C. Latter it decelerates leading to a remainder of 13.5% at 996°C. The temperature of 50% weight loss is 586°C.
- The decomposition occurs according one stage: The processus is ruled by a first-order chemical reaction.

Table 4. Absorbance bands

Absorbance Band Number	Wavenumber (cm^{-1})
1	3481
2	1637
3	1385
4	1125

4.5 Fournier transform infrared spectroscopy

The meaning absorbance bands are displayed in Table 4.

FTIR spectra before aging and after 5000h, 10000h and 15000h are shown in Figure 5 (a-d).

1. It appears an absorbance band at 3481cm^{-1}, assigned to the hydroxyl group OH [20].
2. The absorbance band noticed at 1125cm^{-1} is ascribed to the stretching vibration of ester C-O [20].
3. The absorbance band, located at 1385cm^{-1}, is attributed to the stretching vibration of imide C-N [21].
4. The absorbance band, detected at 1637cm^{-1}, is allocated to the stretching vibration of C=O (Amid I) [22].

4.6 Discussion

1. At long term, water can diffuse through the amorphous regions of the polymer as reported by Hodge et al. [23]. The crystalline regions are considered impermeable. The absorbed water transforms the specimens more polar [24].
2. The change of rupture voltage against aging time is due to the presence of defects before aging (manufacturing) or after exposition of the samples to wet. Its lessening is attributed to a reduction in viscosity expressing a weakening of molecular bonds. Thence, the free volume increases and induces a raise of the mean free path of charge carriers whose mobility grows. Whereas, its growth is assigned to the arranging in the structure. This phenomenon has been reported in a previous work [25]. The decrease attained 51.69% indicating a significant effect of aging time. It was generally agreed that the lifetime-end criterion of polymers is reached when the breakdown voltage decreases to 50% of the initial value.
3. The shape parameter alters versus aging time. The maximum variation is 52.0%. This evolution is allotted to the dimension distribution and the types of defaults within the insulating material. Ueki and Zanin [26] mentioned that the lower the scatter, the higher the shape parameter will be. Its reduction is alloted to the size raise of defects, whereas its augmentation is due to the arrangement in the molecular structure. Coppard et al. [27] reported that the shape parameter is related to the size distribution of the defaults present in polyethylene. Katsuta et al. [28] mentioned that the breakdown voltage decreases versus the dimension of the defaults. The rupture voltage is related to the shape parameter.
4. The breakdown voltage depends on the quantity of space charge restrained in the polymer. In fact, the average value of electrical field applied to the samples is approximately 1MV/cm and space charge can be formed at the interface of the insulation-copper. The attendance of the space charge involves dielectric breakdown of the polymer as yielded by Zhou et al. [29] and Xing et al. [30].
5. Thermogravimetric analysis indicates a change in the beginning temperature of weight loss and a modification of the remainder versus aging time as shown in Figure 4 (a-d).
6. After aging, all the initial infrared absorbance bands appear. Also, new absorbance bands do not arise as shown in Figure 5 (a-d). A short modification, in intensity and width of the absorbance band at 1637cm^{-1}, is observed. It is due to the change of dipole moment of the molecules. We can close that there is no degradation but an alteration of molecular conformation takes place.

5. CONCLUSIONS

1. This investigation indicates that the rupture voltage of the material is affected by hydrolytic aging. The curve of failure voltage against aging time shows several peaks. The increase of failure voltage is attributed to the arrangement in the structure of the polymer. This process reduces the free volume and the mean free path of charge carriers. Its decrease is assigned to the diminution of the viscosity. On the contrary, the free bulk and the mean free path of charge carriers increase. The failure voltage depends on the amount of space charge within the polymer.
2. A modification of the shape parameter against aging time is pointed. The process is linked to the distribution of the defect size. The decrease of the shape parameter can be clarified by the fact that the dimension of defects raises. However, its raise is allotted to the structural arrangement of the polymer.
3. The thermogravimetric analysis shows variations of the onset temperature and the residue of weight with respect to aging time.
4. The infrared spectra indicate no significant change. A The infrared spectra short modification of the spectra is noted at 1637cm^{-1} (C=O stretching of amid I). The results of physical-chemical allow concluding that there is no degradation caused by the hydrolytic aging. The aging induces a changing in the molecular conformation of the material.

REFERENCES

[1] Pelissou, S., Wintle, H.J. (1992). Water content of XLPE cable insulation. In Conference Record of the 1992 IEEE International Symposium on Electrical Insulation, Baltimore, MD, USA, pp. 165-168. https://doi.org/10.1109/ELINSL.1992.247028

[2] Nikolajevic, S.V. (1999). The behavior of water in XLPE and EPR cables and its influence on the electric characteristics of insulation. IEEE Transactions on Power Delivery, 14(1): 39-45. https://doi.org/10.1109/61.736677

[3] Baschek, G., Hartwig, G., Zahradnik, F. (1999). Effect of water absorption in polymers at low and high temperatures. Polymer, 40(12): 3433-3441. https://doi.org/10.1016/S0032-3861(98)00560-6

[4] Crine, J.P., Jow, J. (2005). A water treeing model. IEEE Transactions on Dielectrics and Electrical Insulation, 12(4): 801-808. https://doi.org/10.1109/TDEI.2005.1511105

[5] Nedjar, M., Mecheri, Y., Lamure, A., Aufray, M., Drouet, C. (2010). Effect of moisture on breakdown voltage of polyesterimide used in electrical machines. In 2010 Annual Report Conference on Electrical Insulation and Dielectic Phenomena, West Lafayette, IN, USA, pp. 1-4. https://doi.org/10.1109/CEIDP.2010.5724018

[6] Mecheri, Y., Nedjar, M., Lamure, A., Aufray, M., Drouet, C. (2010). Influence of moisture on the electrical properties of XLPE insulation. In 2010 Annual Report

Conference on Electrical Insulation and Dielectic Phenomena, West Lafayette, IN, USA, pp. 1-4. https://doi.org/10.1109/CEIDP.2010.5724017

[7] Ul-Haq, S. (2003). Influence of moisture on dielectric strength in polyamide (aramid) paper. In 2003 Annual Report Conference on Electrical Insulation and Dielectric Phenomena, Albuquerque, NM, USA, pp. 325-328. https://doi.org/10.1109/CEIDP.2003.1254859

[8] Chauvet, C., Laurent, C., Mayoux, C. (1989). Influence of wet ageing on the electrical breakdown strength of XLPE cable slices. In Conference on Electrical Insulation and Dielectric Phenomena, Leesburg, VA, USA, pp. 230-234. https://doi.org/10.1109/CEIDP.1989.69551

[9] Diaz, C.M., Gao, X., Robisson, A., Amarante, M., Zhu, S.S. (2018). Effect of hydrolytic degradation on the mechanical property of a thermoplastic polyether ester elastomer. Polymer Degradation and Stability, 155: 35-42. https://doi.org/10.1016/j.polymdegradstab.2018.07.002

[10] Ueda, K. (1989). Progress of magnet wire technology in Japan. IEEE Electrical Insulation Magazine, 5(3): 18-26. https://doi.org/10.1109/57.32445

[11] Wires, W. (2008). Winding wires: Test methods-part 5: Electrical properties. 4th Edition. IEC Standard, 60851-5.

[12] Dissado, L.A., Fothergill, J.C. (1992). Electrical Degradation and Breakdown in Polymers. The Institution of Engineering and Technology.

[13] Diaham, S., Zelmat, S., Locatelli, M.L., Dinculescu, S., Decup, M., Lebey, T. (2010). Dielectric breakdown of polyimide films: Area, thickness and temperature dependence. IEEE Transactions on Dielectrics and Electrical Insulation, 17(1): 18-27. https://doi.org/10.1109/TDEI.2010.5411997

[14] Nedjar, M. (2022). Breakdown behaviour of polyesterimide enamelled wire subjected to thermal aging. Annales de Chimie Science des Matériaux, 46(3): 163-168. https://doi.org/10.18280/acsm.460308

[15] Ben Saidj, I., Nedjar, M., Hocine, S., Belabbas, F. (2022). Effects of hydrothermal aging on the breakdown voltage of polyesterimide. Annales de Chimie Science des Matériaux, 46(2): 95-102. https://doi.org/10.18280/acsm.460205

[16] Nedjar, M., Ould Ouali, S.H. (2011). Statistical investigation of short-term dielectric breakdown of polyesterimide and polyamide imide used in electrical machines. Annales de Chimie Science des Matériaux, 36(2): 59-72. https://doi.org/10.3166/acsm.36.59-72

[17] Stone, G.C., Van Heeswijk, R.G. (1977). Parameter estimation for the Weibull distribution. IEEE Transactions on Electrical Insulation, EI-12(4): 253-261. https://doi.org/10.1109/TEI.1977.297976

[18] IEEE. (1987). IEEE guide for the statistical analysis of electrical insulation voltage endurance data. In ANSI/IEEE Std 930-1987, pp. 1-28 https://doi.org/10.1109/IEEESTD.1987.86250

[19] Jacquelin, J. (1993). Generalization of the method of maximum likelihood (insulation testing). IEEE Transactions on Electrical Insulation, 28(1): 65-72. https://doi.org/10.1109/14.192241

[20] Silverstein, R.M., Webster, F.X., Kiemle, D.J. (2005). Spectroscopic Identification of Organic Compounds. John Wiley & Sons, 7th edition.

[21] Tseng, I.H., Liao, Y.F., Chiang, J.C., Tsai, M.H. (2012). Transparent polyimide/graphene oxide nanocomposite with improved moisture barrier property. Materials Chemistry and Physics, 136(1): 247-253. https://doi.org/10.1016/j.matchemphys.2012.06.061

[22] Chércoles Asensio, R., San Andrés Moya, M., De la Roja, J.M., Gómez, M. (2009). Analytical characterization of polymers used in conservation and restoration by ATR-FTIR spectroscopy. Analytical and Bioanalytical Chemistry, 395: 2081-2096. https://doi.org/10.1007/s00216-009-3201-2.

[23] Hodge, R.M., Edward, G.H., Simon, G.P. (1996). Water absorption and states of water in semicrystalline poly (vinyl alcohol) films. Polymer, 37(8): 1371-1376. https://doi.org/10.1016/0032-3861(96)81134-7

[24] Van Krevelen, D.W. (1976) Properties of Polymers. Elsevier, New York, second Edition.

[25] Ait-Saadi, Z., Nedjar, M. (2023). Electrical properties of polyethylene terephthalate under hydrothermal aging. Mathematical Modelling of Engineering Problems, 10(1): 63-70. https://doi.org/10.18280/mmep.100108

[26] Ueki, M.M., Zanin, M. (1999). Influence of additives on the dielectric strength of high-density polyethylene. IEEE Transactions on Dielectrics and Electrical Insulation, 6(6): 876-881. https://doi.org/10.1109/94.822030

[27] Coppard, R.W., Bowman, J., Dissado, L.A., Rowland, S.M., Rakowski, R.T. (1990). The effect of aluminium inclusions on the dielectric breakdown of polyethylene. Journal of Physics D: Applied Physics, 23: 1554. https://doi.org/10.1088/0022-3727/23/12/011

[28] Katsuta, G., Toya, A., Katakai, S., Kanaoka, M., Sekii, Y. (1991). Influence of defects on insulating properties of XLPE cable. In Proceedings of the 3rd International Conference on Properties and Applications of Dielectric Materials, Tokyo, Japan, pp. 485-489. https://doi.org/10.1109/ICPADM.1991.172103

[29] Zhou, C., Chen, G. (2017). Space charge and AC electrical breakdown strength in polyethylene. IEEE Transactions on Dielectrics and Electrical Insulation, 24(1): 559-566. https://doi.org/10.1109/CEIDP.2015.7352027

[30] Xing, Z.L., Gu, Z.L., Zhang, C., Guo, S.W., Cui, H.Z., Lei, Q.Q., Li, G.C. (2022). Influence of space charge on dielectric property and breakdown strength of polypropylene dielectrics under strong electric field. Energies, 15(12): 4412. https://doi.org/10.3390/en15124412